HHS Public Access

Author manuscript

Nat Neurosci. Author manuscript; available in PMC 2013 June 01.

Published in final edited form as:

Nat Neurosci. 2012 December ; 15(12): 1700–1706. doi:10.1038/nn.3260.

Optical controlling reveals time-dependent roles for adult-born dentate granule cells

Yan Gu[1], **Maithe Arruda-Carvalho**[3,4], **Jia Wang**[1], **Stephen Janoschka**[1,2], **Sheena Josselyn**[3,4,5], **Paul Frankland**[3,4,5,*], and **Shaoyu Ge**[1,2,*]

[1]Department of Neurobiology and Behavior, SUNY at Stony Brook, Stony Brook, NY 11794

[2]Program in Neuroscience, SUNY at Stony Brook, Stony Brook, NY 11794

[3]Program in Neurosciences and Mental Health, Hospital for Sick Children, 555 University Ave, Toronto, Ontario, Canada, M5G 1X8

[4]Institute of Medical Science, University of Toronto, Toronto, Ontario, Canada, M5S 1A8

[5]Department of Physiology, University of Toronto, Toronto, Ontario, Canada, M5S 1A8

Abstract

Accumulating evidence suggests that global depletion of adult hippocampal neurogenesis influences its function and the timing of the depletion impacts the deficits. However, behavioral roles of adult-born neurons during their establishment of projections to CA3 pyramidal neurons remain largely unknown. Here we combined retroviral and optogenetic approaches to birth-date and reversibly control a group of adult-born neurons in adult mice. We show that adult-born neurons form functional synapses on CA3 pyramidal neurons as early as 2 weeks after birth, and that this projection to the CA3 area becomes stable by 4 weeks in age. Newborn neurons at this age exhibit enhanced plasticity compared to other stages. Notably, we found that reversibly silencing this cohort of ~4 week-old cells after training, but not cells of other ages, substantially disrupted retrieval of hippocampal memory. Our results identify a restricted time window for adult-born neurons exhibiting an essential role in hippocampal memory retrieval.

Introduction

The adult hippocampus continues to give rise to several thousand new dentate granule cells each day [1–3]. Accumulating evidence from studies using global perturbation or ablation of adult hippocampal neurogenesis has revealed deficits in some forms of hippocampal

*Correspondence can be addressed to: Shaoyu Ge Ph.D., Department of Neurobiology and Behavior, SUNY at Stony Brook, Stony Brook, NY 11794, USA, sge@notes.cc.sunysb.edu, Tel: 631-632-8799, Fax: 631-632-6661 Or Paul Frankland Ph.D., Hospital for Sick Children, Neurosciences & Mental Health, Hospital for Sick Children, Toronto, Ontario, Canada, M5G 1X8, paul.frankland@sickkids.ca, Tel: 416-813-7654 x1823, Fax: 416-813-7717.

Author contributions

Y.G. conducted all electrophysiological, immunohistochemical and confocal imaging analysis. Y.G. and M.A.-C. performed all behavioral analysis. J.W. engineered retroviral constructs and Y.G. produced retrovirus. S.J helped on some initial manuscript preparation. S.G. and P.W.F. supervised the project. S.G., P.W.F., S.A.J., Y.G. and M.A.-C. wrote the manuscript. All authors read and discussed the manuscript.

memory in rodents [4–9]. As the morphological and physiological phenotypes of adult-born cells change dramatically as they mature, they may play distinct roles at different stages following integration into hippocampal circuits. Accordingly, while traditional manipulations of adult neurogenesis may disrupt hippocampal memory function, it is not clear whether the observed memory deficits are due to a global disruption of neurogenesis.

Emerging evidence has shown that surviving adult-born dentate granule cells (DGCs) extend dendrites and receive functional input from the existing neural circuits as early as 2 weeks after birth [10–14]. In contrast to many studies on input synapses, little is known about the establishment of functional projection of adult-born DGCs to the hippocampal trisynaptic circuit. Although massive effort has been put into determining output circuit formation of adult-born neurons, most evidence is from anatomical examinations showing that young newborn DGCs gradually extend axonal fibers into the CA3 area. Two to three weeks after birth, terminals of these axons form bouton-like structures similar to mature granule cells [15–18]. A recent study demonstrated that mature newborn neurons exhibit synaptic responses in the CA3 area [16]. However, the precise timing for functional output synapse formation and maturation remains unknown.

Input (dendritic) synapses of adult-born neurons show enhanced plasticity between 4–6 weeks after birth compared to other stages [19], during which time they exhibit heightened intrinsic excitability and lower activation threshold [13,20]. This coincides with the timing when newborn neurons are recruited into adult neural circuits mediating behavior [21–23]. These findings suggest that a cohort of young adult-born neurons of similar age may form a hypersensitive unit that preferentially responds to stimuli during hippocampal memory formation. A related interesting question is whether output synapses, if formed and functional, also exhibit heightened plasticity around the same time.

Combining retroviral birth-dating and gene delivery [10–11] with optogenetic stimulation [24], here we examined the behavioral roles of adult-born neurons during their output circuit development. We found that adult-born DGCs establish functional synapses with CA3 pyramidal neurons as early as 2 weeks after birth and synaptic responses become stable by ~4 weeks in age. Fully established output synapses of adult-born neurons exhibit enhanced plasticity at ~4 weeks after birth. Importantly, optogenetic silencing of a cohort of 4 but not 2 or 8 weeks old newborn neurons substantially impacted the retrieval of hippocampal dependent memory following the completion of training, suggesting that 4 week-old new neurons play a privileged role in hippocampal memory function. These data characterize the development of output circuit function for adult-born DGCs, revealing a precise time window where newborn neurons exhibit enhanced plasticity at CA3 synapses and play a critical role in processing hippocampal memories.

Results

Establishment of output synapses of adult-born neurons

To examine a role of adult-born neurons in hippocampal function during their circuit integration, we first determined the timing for newborn neurons to establish functional projections to CA3 pyramidal neurons. We elected to use an optogenetic method to excite a

group of adult-born DGCs simultaneously to determine the development of functional output circuit in the CA3 area [16,24]. We constructed a retroviral vector expressing EGFP-tagged Channelrhodopsin 2 (ChR2-EGFP), a gene encoding a light-sensitive channel [24–25], to birth-date and specifically express ChR2-EGFP in adult-born hippocampal neurons [10–11,16]. ChR2-EGFP retroviruses were microinjected into the hilus of the dentate gyrus in adult mice and acute brain sections were prepared 1–8 weeks post infection (wpi) (Fig. 1a; Supplementary Fig. 1a, b; Methods; [11]). As expected, ChR2-EGFP retroviruses specifically targeted neural progenitors and these cells gradually developed into typical DGCs (Supplementary Fig. 1c–e). Importantly, brief pulses of blue light reliably induced action potentials in infected DGCs but not in non-infected neighbors (Fig. 1b), indicating that this population of cells could be optically controlled. The infected cells were not illuminated during development, and we did not observe changes in intrinsic properties of newborn neurons expressing ChR2 at different ages compared to those expressing EGFP only (Supplementary Table 1), consistent with previous findings where optogenes have been expressed in other cell types [24].

Next, we used whole-cell recording to examine postsynaptic currents in CA3 pyramidal neurons while optically stimulating ChR2-EGFP positive mossy fibers of newborn DGCs (Fig. 1c). Postsynaptic activity increased with the age of infected adult born DGCs (Fig. 1d). At 1 wpi, a time-point when mossy fibers have not yet reached the CA3 region, no postsynaptic responses were observed following optical stimulation. However, at 2 wpi and older (a stage when mossy fibers have reached the CA3 region), stimulation produced excitatory postsynaptic responses (EPSCs). These optically evoked EPSCs reached maximal responses at 4 wpi (Fig. 1d, e). They had a latency of ~4ms, and were blocked by an AMPA receptor antagonist (CNQX) and metabotropic glutamate receptor agonists (L-AP4 and LY354740, specifically blocking mossy fiber-CA3 synapses [26]), indicating a glutamatergic mono-synaptic response (Fig. 1f, g). These results show young adult-born DGCs form functional synapses with CA3 target cells which become stable around 4 wpi. These current results, together with previous studies showing newborn neurons to be functionally innervated by entorhinal cortical projections [10–12], indicate that adult-born DGCs fully integrate into the hippocampal trisynaptic circuits by ~4 wpi.

Heightened synaptic plasticity of young adult-born neurons

We next characterized functional properties of these output synapses. We examined synaptic plasticity of young adult-born DGCs in the CA3, as previously described [13,19]. To optically stimulate CA3 synapses of a group of adult-born neurons at high frequency, we replaced the ChR2 construct with a ChR2 variant ChIEF-dTomato [27], which responds more reliably to high frequency optical stimulation. As expected, 3, 4 and 8 week-old adult-born DGCs expressing ChIEF responded reliably to a theta-burst optical stimulation (TBS), a paradigm used for long-term potentiation (LTP) induction (Supplementary Fig. 2a; [13,19,27–28]), to their soma (Supplementary Fig. 2b, c). Recordings from axonal boutons indicated that following optical stimulation activation in soma could reliably propagate to the axonal terminals (Supplementary Fig. 2d, e), consistent with previous observations in mature DGCs [29]. To assess global circuit output of newborn neurons, we then implanted an optic fiber in the dentate gyrus to deliver optical stimulation and recorded field excitatory postsynaptic

potentials (fEPSPs) in the CA3 region *in vivo* (Fig. 2a; Supplementary Fig. 3). fEPSPs were successfully induced by short pulses of optical stimulation (Fig. 2b). Similar to postsynaptic activity *in vitro* (Fig. 1c), fEPSPs recorded *in vivo* were blocked by local application of CNQX (Fig. 2b). As expected, high frequency optical stimulation (~5 mW/mm^2 intensity, 50 Hz, 2 s) evoked consistent fEPSPs (Fig. 2b). Together with the reliable responses to TBS recorded from the soma or axonal terminals of newborn neurons (Supplementary Fig. 2), this result suggests that the experimental system is suitable for characterizing output synaptic plasticity of newborn DGCs using TBSTherefore, we next delivered TBS, and measured fEPSPs slope before and after the TBS (Methods; [19]). We found that optical TBS at 3 and 4 wpi induced LTP of fEPSPs in the CA3 area in nearly all tested animals (Fig. 2c, d). When the same induction paradigm was used to induce LTP at 8 wpi, only half of tested animals exhibited potentiation (Fig. 2c, d). Therefore, output synapses of adult-born DGCs at 4 wpi exhibit a lower induction threshold for LTP, similar to their input synapses [13,19]. We then analyzed LTP amplitude at 3, 4, and 8 wpi, and found that LTP amplitude was maximal at 4 weeks. Relatively smaller LTP was observed in mice that were stimulated at 3 and 8 wpi (Fig. 2c, e). To determine whether the substantially reduced LTP at 8 wpi resulted from lack of plasticity in the output synapses of newborn neurons around this age, we used a stronger induction paradigm, tetanic optical stimulation (50 Hz, 2 s), for LTP induction while recording pyramidal cells (Supplementary Fig. 4a). As shown in Supplementary Fig. 4b, c, we recorded sustained potentiation following this stronger induction protocol, suggesting the output synapses of mature newborn DGCs remain plastic but have a higher induction threshold. However, using the same tetanic optical stimulation, we found a substantially higher level of LTP expression by stimulating young newborn neurons compared to that induced by stimulating mature newborn neurons (Supplementary Fig. 4b–d), consistent with our observation using theta-burst induction in Fig. 2. Our results here indicate that young newborn neurons exhibit heightened plasticity that peaks at ~4 wpi (Fig. 2e).

We next asked what might contribute to the heightened plasticity in young newborn neurons. A recent study found that T-type Ca^{2+} channels facilitate dendritic synaptic plasticity in young newborn (but not mature) DGCs[13]. Accordingly, we next examined whether the activity of T-type Ca^{2+} channels contributed to the heightened plasticity. After establishing reliable recordings from the animals at 3, 4 and 8 wpi, we blocked T-type Ca^{2+} channels with intraperitoneal (i.p.) injection of mibefradil (25mg/kg), a specific T-type Ca^{2+} channel blocker, and examined their role in the expression of output synaptic plasticity (Methods; [30]). Mibefradil showed no effect on the basal synaptic transmission (Supplementary Fig. 5a, b). Notably, optical TBS failed to induce an enhancement of synaptic transmission from mibefradil-treated animals at 3 and 4 wpi (Fig. 2e), at which we observed robust potentiation in control animals using the same induction paradigm (Fig. 2e). Although mibefradil is considered a specific blocker, it has been reported to block R-type Ca^{2+} channels of some cultured cells at low dose [31]. To exclude this possibility, we performed recordings in hippocampal slices from mice at ~4wpi. Consistent with our *in vivo* data, application of mibefradil (1 μM) abolished LTP of young DGCs, while SNX482 (500nM), an R-type specific antagonist, failed to affect this LTP (Supplementary Fig. 5c–f). From mibefradil-treated animals at ~8 wpi, LTP seemed to be unaffected by mibefradil

application. Because of the small LTP expression using TBS at this age, we were unable to determine precisely (Fig. 2e). However, together with previous observation of specific activation of T-type Ca^{2+} channels in young neurons [13], these data suggest the activity of T-type Ca^{2+} channels in young adult-born DGCs likely contributes to the heightened output synaptic LTP. With previous studies on intrinsic excitability and input synapses [13,19,32], these results reveal that a cohort of fully-integrated (~4 weeks old) young newborn DGCs have more excitable membranes and enhanced input/output synaptic plasticity.

Silencing young newborn neurons affects memory retrieval

Accumulating evidence suggests that the effectiveness of ablations of adult neurogenesis depend on the timing of manipulation [2,5,7–8,23]. This suggests that as adult-born DGCs mature they may assume distinct behavioral roles, and these distinct behavioral roles may coincide with changes in their synaptic integration and plasticity (Fig. 2e). To test this hypothesis, we used optogenetic stimulation to reversibly silence groups of different aged adult-born neurons during behavioral tasks. We generated a retrovirus to express inhibitory optogene, archaerhodopsin-3 (Arch-EGFP; [33]). To maximize infection of adult-born neurons, we performed two retroviral injections (spaced 10 hrs apart) per animal using a standard protocol as (Methods, [11]). We successfully labeled ~1700 newborn DGCs per animal at 4 wpi. The Arch expression in labeled adult-born DGCs showed no observable effect on the development of newborn neurons as shown in Supplementary Table 1. In acutely prepared brain sections, pulses of optical stimulation specifically silenced Arch expressing adult-born DGCs, indicating that the activity of these neurons can be reliably and reversibly inhibited by light (Fig. 3a), as previously reported [33].

To examine the role of a group of newborn neurons in hippocampal memory, we used a hidden platform version of the water maze task [34]. We microinjected Arch retroviruses into the hilus of the hippocampus in adult mice, and implanted customized optrodes to ensure sufficient light delivery into the dorsal hippocampus bilaterally (Methods; Supplementary Fig. 6). At 4 wpi, mice were trained in the water maze with optic fibers connected to an orange light source via an optic-rotatory joint. Half the mice were trained with light off (“no light” group) and half with light on (“light” group) during training (Fig. 3b, Supplementary Fig. 7a). Across the training trials, latencies to locate the hidden platform declined, and there was no difference in escape latencies between control (no light) and inactivated (light) groups (Supplementary Fig. 7b), indicating that silencing this cohort of ~4 week-old adult-born DGCs does not interfere with memory acquisition.

We then assessed the effect of silencing newborn neurons on memory retrieval. Similar to before, at ~4 wpi, mice were trained in the water maze with optic fibers connected to an inactive light source (“no light”), and the mice learnt to locate the hidden platform (Fig. 3b–d). Following the completion of training, spatial memory was assessed in two probe tests. During the first probe, half the animals received light stimulation for the duration of the test (“light”) and half were tested without the light (“no light”). On the following day, the animals were re-tested in a second probe trial with the light conditions reversed (Fig. 3c, d). Using this within-subject design, we found that inactivation of this cohort of 4 weeks old adult-born neurons robustly decreased the percent time that the mice spent searching in the

target quadrant (Fig. 3e). Importantly, light illumination of 4 week-old EGFP-labeled newborn neurons did not affect the percent time in the target quadrant (Supplementary Fig. 8). Furthermore, light-induced inactivation did not impact motor coordination, as swim speed (Fig. 3f) and distance traveled (Fig. 3g) did not differ between “no light” and “light” conditions. Memory impairments depended upon both retroviral expression of Arch and light illumination since neither retroviral expression of Arch alone (without illumination) nor illumination alone (in the absence of Arch) impaired memory (Supplementary Fig. 8; [10]). These results suggest that a cohort of ~4 week-old newborn cells plays a key role in memory expression. By examining expression of the activity-regulated gene, c-fos, we next asked whether this population of cells was normally activated by memory recall, and whether this activation was absent following light-induced inactivation. Mice received injections of Arch or EGFP retrovirus into the dentate, and 4 weeks later were trained in the water maze. At the completion of training, half the mice were given a probe test with the light on and the other half with no light (Supplementary Fig. 9a). Using standard procedures [21], 90 minutes after the probe tests, we sacrificed the mice and performed c-fos staining. We imaged c-fos+ and EGFP+/Arch+ DGCs (Supplementary Fig. 9b). Mice in the Arch/no light and EGFP groups searched selectively in the probe test, as expected. Following this probe test, we found about 4% of labeled adult-born DGCs were c-fos positive (Supplementary Fig. 9c), consistent with our previous findings [21]. In contrast, mice in the Arch/light group searched less selectively in the probe test (similar to deficits observed in Fig. 3d), and very few Arch-labeled adult-born DGCs expressed c-fos (Supplementary Fig. 9b, c), confirming the efficiency of optical inhibition, and additionally, providing support for the conclusion that labeled ~ 4 week-old adult-born DGCs regulate spatial memory retrieval.

We next evaluated whether silencing these neurons interfered with the expression of a non-hippocampus-dependent memory. The same mice were trained in a visible version of the water maze in which the platform was located in the opposite quadrant of the pool and marked by a visible cue. Across two days of training, mice learned to navigate to the cue from different start positions (Fig. 3c, d). During two subsequent probe tests, we found that light inactivation did not interfere with the laterncy of the mice to find the visible platform (No light: 4.92±0.26 s; Light: 4.87±0.34 s; t=0.1215, p=0.4526; n=14; two-tailed unpaired t-test), swimming (Fig. 3f) or distance traveled (Fig. 3g).

To ask whether our results would generalize to another form of hippocampus-dependent memory, we next trained a new group of animals in a fear conditioning paradigm (Fig. 4a, [35]). Mice were trained with a single tone-shock pairing and tested in the same context one day later. In this test, optogenetic silencing reduced levels of conditioned freezing (Fig. 4b, c), indicating that inactivating 4 week-old adult-born neurons impaired the retrieval of contextual fear memory. The following day, we placed the mice in an alternate context and preseneted the tone. In contrast, optogenetically silencing these neurons did not affect conditioned freezing of the mice to the tone (Fig. 4c). As the retrieval of contextual, but not tone, fear memories depends on hippocampal function [35], these results suggest that silencing a cohort of 4 week-old adult-born DGCs impaired retrieval of a hippocampus-dependent contextual fear memory.

The behavioral role for newborn DGCs relies on their age

We next asked whether silencing different aged cohorts of newborn neurons would have similar impact on hippocampal memory retrieval. To address this, we trained mice at 2 or 8 wpi. Silencing cells that were ~2 weeks-old at the time of training did not disrupt expression of spatial memory (Fig. 5a). Similarly, silencing cells that were ~8 weeks old at the time of training, an age at which they are considered mature (Fig. 1, [11–12,17]), did not affect expression of a spatial memory (Fig. 5b). Therefore, silencing newborn neurons at ~4wpi, but not at 2wpi or 8wpi, caused deficits in spatial memory retrieval (Fig. 5c). Furthermore, silencing newborn neurons at 2 or 8 wpi did not affect context fear memory (Fig. 5d).

Not all adult-born DGCs survive and therefore the absence of effects of silencing at 8 weeks might be because there are fewer Arch+ cells. Accordingly, we counted Arch positive newborn DGCs after behavioral tests. We found that there was no obvious decrease in number of Arch-labeled neurons from 4 to 8 wpi (4 wpi: 1746±52 labeled neurons per animal, n=17; 8 wpi: 1721±59 labeled neurons per animal, n=10; p=0.23, two-tailed unpaired t-test), consistent with previous studies [1,4,36]. Furthermore, we found Arch+ cells had similar dendritic complexity ~4 and 8 wpi (4 wpi: 9.85±1.08 dendrites/50μm×50μm; 8 wpi: 10.27±0.95 dendrites/50μm×50μm; p=0.78; n=17, 10; two-tailed unpaired t-test).

Finally, we asked whether the coincidently heightened plasticity (Fig. 2) contributes to the role of young newborn neurons in retrieval of hippocampal-dependent memories. Since we found that the activity of T-type Ca^{2+} channels plays an essential role in the heightened plasticity of output synapses, we tested hippocampal memory of the Arch-injected animals at 4 wpi with i.p. administration of mibefradil (25mg/kg). Notably, the application of mibefradil substantially decreased the searching time in the target quadrant compared to the saline-no light groups (Fig. 5e). In another group of animals, when we applied mibefradil and optical inhibition, we observed a similar deficit in memory retrieval in the mibefradil treated animals (Fig. 5e). Because the activity of T-type Ca^{2+} channels is also required for the heightened plasticity in dendritic synapses [13], these data suggest that heightened plasticity in young newborn neurons may play a key role in memory retrieval. To further explore the age-specificity of these effects in the same cohort of newborn neurons, we designed a within subject experiment where mice were tested water maze at 4 wpi and contextual fear conditioning at 8 wpi, or vice versa (Fig. 6). We found that silencing newborn neurons at 4 wpi, but not 8 wpi, disrupted memory retrieval in both tasks, consistent with our above observations (Fig. 3–5). Together, our data suggest that adult-born neurons may transiently play a critical role in memory retrieval, but the impact, at least in spatial and contextual memory retrieval, may decline as these adult-born neurons continue to mature.

Discussion

We used optogenetic methods to evaluate how adult-born DGCs functionally integrate into hippocampal circuits. We found that newborn DGCs form functional glutamatergic synapses in the CA3 area as early as 2 wpi and these synapses become functionally stable by 4 wpi. The output synapses of 4-week old newborn neurons exhibit enhanced plasticity. Notably, reversibly silencing a population of 4 but not 2 or 8 weeks old newborn DGCs impacted

hippocampal memory retrieval. These data indicate that adult-born neurons influence hippocampal function and behaviors in a maturation-dependent manner.

Functional output circuit development

In the current study, we successfully employed retroviral method to deliver optogenes into cohorts of adult-born DGCs. As we previously reported [10–11], infection with these retroviruses did not appear to affect the development of labeled newborn neurons (Supplementary Fig. 1 and Table 1). By using optogenetic stimulation, physiology and imaging methods, we established that adult-born neurons functionally project to the CA3 neural circuitry. Blockade of post synaptic responses by applying AMPA receptor antagonists or metabotropic glutamate receptor agonists suggests that they are typical mossy fiber synapses(Fig. 1e; [26]). Together with several previous studies [10–12,17], our study reveals that adult-born DGCs fully incorporate into the hippocampal trisynaptic neural circuit around 4 wpi.

We further found output synapses of adult-born DGCs exhibit enhanced plasticity at ~4 wpi (Fig. 2). This mirrors the time during which we observed hyper-sensitive input synapses, and when these cells have more excitable membranes [13,19]. Mechanistically, we found that mibefradil, a T-type Ca^{2+} channel blocker, could abolish the heightened axonal plasticity of young newborn neurons, similar to its effect on their dendritic synapses [13]. Although it is possible that mibefradil affects R-type Ca^{2+} channels [31], heightened plasticity was not blocked by the application of SNX-482, an R-type Ca^{2+} channel antagonist. Considering previous studies showing its specificity [30,37–38] and young DGCs representing a hyperactive population with high-level T-type Ca^{2+} channels [13], we think T-type Ca^{2+} channels are very likely the major targets of mibefradil. Additionally, the mechanisms described in the dendritic synapses of adult-born DGCs [19, 26,39, 20] may contribute to the heighted axonal plasticity [40]. Although the precise mechanisms remain to be determined, impaired spatial memory following blockade of T-type channels suggest that these channels play important functional roles in adult-born neurons.

Time-dependent role of young adult-born neurons

Chemical, genetic and irradiation-based methods have been widely used to ablate neurogenesis and explore the role of adult neurogenesis in hippocampal function [5,41]. While these studies suggest that adult neurogenesis plays an important role in hippocampal memory, a limitation is that these manipulations typically affect differently aged adult-born cells. By retrovirally expressing optogenes we were able to address this issue by labeling and silencing distinct cohorts of adult-born neurons. This optogenetic silencing of adult-born neurons by high frequency light stimulation is likely to result from “effective but not excessive” hyperpolarization, rather than potentially harmful changes in internal chloride levels [33].

Our experiments indicated that silencing of ~4 week-old newborn neurons led to memory deficits. In contrast silencing this same population before training did not prevent the acquisition of a hippocampal memory. The dissociation is consistent with our recent findings using a transgenic diphtheria toxin-based ablation system to study role of adult-

born neurons in hippocampal memory [7], and suggests that learning may occur in the absence of newborn neurons. However, if newborn neurons are present and functional in circuit level at the time of training, they are recruited into hippocampal memory circuits and silencing (or ablating [7]) these cells reveals that they play an essential role in memory retrieval. In our previous diphtheria toxin-based ablation study, adult-born cells spanning a range of ages (including ~4 week-old cells) were targeted [7]. The present finding that while substantial memory retrieval deficits were only observed after silencing of ~4 week-old newborn neurons, raises the possibility that the deficits following post-training ablation in our previous study were primarily driven by loss of ~4 week-old newborn neurons. Still, we cannot exclude the possibility that silencing ~8 week-old newborn neurons also impacts hippocampal function, albeit to a lesser degree. Finally, it is noteworthy that the retroviral approach only labels a relatively small group of newborn neurons, and so even the activity of this small population of cells strongly influences hippocampal function. While silencing a similar population before training did not impair memory acquisition, it is likely that silencing a larger population might induce anterograde memory deficits.

Methods

Retroviral production and stereotaxic injection

Engineered self-inactivating murine oncoretroviruses were used to deliver genes of interest specifically to proliferating cells and their progeny [10–11]. The optimized ChR2 constructs were obtained from Karl Deisseroth and ChIEF construct from Roger Tsien (Addgene). The Arch construct from Edward Boyden was purchased from Addgene.

Purified engineered retroviruses were stereotaxically injected into adult C57BL/6 mice (Charles River). 5–6 weeks old female mice were used for all experiments. For behavioral experiments, animals in each experimental group in general had slight different birthdates to minimize the potential effects from the estrous cycle. All mice were housed under standard conditions with 12 hr:12 hr dark/light cycle. All animal procedures were conducted in accordance with institutional guidelines and were approved by the ethical committee.

Optrode implantation and behavioral procedures

Optrodes (Doric Lenses Inc., Canada, modified to increase light spread) were implanted bilaterally into the dorsal dentate gyrus (coordinates: 3.0 mm rostral from bregma, 2.6 mm lateral from the midline and 2.5 mm ventral) 14 days after two retroviral injections (~10 hours interval) unless we specifically addressed in the main text. After implantation, animals received at least 2 weeks recovery before any behavioral experiment.

After behavioral experiments, mice were perfused transcardially with PBS followed by 4% PFA. Brains were sectioned and the optrode implantation sites were verified and numbers of retroviral-labeled adult-born neurons were counted. Mice were excluded if the implantation site was incorrectly positioned. Mice with missed viral injections were discarded. Mice with correct injections all had 1500 ~2000 newborn DGCs and all of them have been selected for behavioral analysis.

Water maze (hidden platform version)—The apparatus and behavioral procedures have been previously described [21,42]. Behavioral testing was conducted in a circular water maze tank (120cm in diameter, 50cm deep), located in a dimly-lit room. The pool was filled to a depth of 40cm with water made opaque by adding white, non-toxic paint. Water temperature was maintained at approximately 26°C. A circular escape platform (10 cm diameter) was submerged 0.5 cm below the water surface, in a fixed position in one of the quadrants. The pool was surrounded by curtains, at least 1 m from the perimeter of the pool. The curtains were white with distinct cues painted on them.

Water maze training took place across 6 days. Each training session consisted of 3 training trials (inter-trial interval was ~15 s). On each trial, mice were placed into the pool, facing the wall, in one of 4 pseudorandomly-varied start locations. The trial was complete once the mouse found the platform or 40 seconds had elapsed. If the mouse failed to find the platform on a given trial, it was guided onto the platform by the experimenter. Following training, spatial memory was assessed in two probe tests with the platform removed from the pool. The probe tests were 40 s in duration and conducted 24 h and 48 h after the last training session. Animals performed training and probes attached to the optic fibers and rotatory joint. Each animal experienced one probe with light stimulation and one without, the order of which was counterbalanced between animals. Behavioral data from training and the probe tests were acquired and analyzed using an automated tracking system (Ethovision XT, Noldus, Wageningen, Netherlands). Using this software, we recorded a number of parameters during training, including escape latency and swim speed. In probe tests, we measured the amount of time mice searched in the target quadrant vs. the three other quadrants.

Water maze (visible platform version)—For the visible platform task, the platform was moved to the opposite quadrant and marked by a visual cue. The cue consisted of a plastic cylinder (4 cm in diameter, 4 cm in height) with a horizontal black/white vertical striped pattern and was placed on top of the platform. Visible platform training started 24h after the last hidden platform probe and consisted of one training session of 3 trials per day (inter-trial interval was ~15 s) across two days. On each trial mice were placed into the pool, facing the wall, in one of 4 start locations (pseudorandomly-varied). The trial was complete once the mouse found the escape platform or 40 s had elapsed. Similar to the hidden version of the water maze, animals were divided into two groups to perform two probe tests, counterbalanced for order of light stimulation. The probes started 24h after training and were conducted on consecutive days. As before, behavioral data from training and the probe tests were acquired and analyzed using an automated tracking system.

Context fear conditioning—The fear conditioning chamber consisted of a stainless steel conditioning chamber (18 cm × 18 cm × 30 cm; Coulbourn, Whitehall, PA), containing a stainless steel shock-grid floor. Shock grid bars (diameter 3.2 mm) were spaced 7.9 mm apart. The grid floor was positioned over a plastic drop-pan, which was lightly cleaned with 70% ethyl alcohol to provide a background odor. The front of the chamber was made of clear acrylic and the top, back and two sides made of modular aluminum. Animals were subjected to two probes, a context test and a tone test. For the context testing animals were

placed in the fear chamber, where they were originally shocked. For tone testing mice were put in a modified version of the fear chamber that consisted of a white, plastic floor covering the shock grid bars and a plastic, triangular insert placed inside the same conditioning chamber used for training. One of the walls of this insert had a black/white striped pattern. The other two walls were white. After each test the plastic floor was cleaned with water. Mouse freezing behavior was monitored via overhead cameras and scored manually.

During training, mice were placed in the fear conditioning chamber for a total of 3 min. After 2 min of free exploration mice were presented with a 30 s tone (2800 Hz, 85 dB) that coterminated with a 2 s footshock (0.5 mA). Mice remained in the chamber for a further 30 s before being returned to their home cage.

Twenty four hours after training, freezing was assessed in two 5 min tests, in the fear chamber and its modified version, respectively. In the second probe, the tone was presented after a 2 min delay. Animals were divided into two groups for counterbalanced tests of the animals's freezing to the context and the tone, respectively. Data is presented as function of time for the context test. For the tone test we measured freezing to the tone for 60 seconds.

Slice and *in vivo* physiology

Mice were processed at 1, 2, 3 and 4 wpi and electrophysiological recordings performed at 32°C – 34°C, as previously described [11]. For efferent CA3 synapse slice experiments, short pulses of blue light were generated by a 50 mW 473 nm laser under the control of a standard TTL board and launched into a Zeiss upright microscope through the epifluorescence light path. The ending power on brain slices was ~5 mW/mm^2 and synaptic transmission was recorded at −65mV.

For *in vivo* recording, mice received injections of ChIEF-dTomato retrovirus 3, 4 and 8 weeks prior to *in vivo* recordings. Briefly, animals were anesthetized and mounted on a stereotaxic frame. An optrode was inserted into dorsal dentate gyrus (coordinates: 3.0 mm rostral from bregma, 2.6 mm lateral from the midline and 2.5 mm ventral). Pulses of blue light controlled by recording software (pClamp10.0) was generated from a 50mW 473nm laser and delivered thought an optic fiber. A recording electrode was inserted into CA3 molecular layer (coordinates: 2.0mm rostral from bregma, 2.2mm lateral from the midline and 2.2mm ventral), and field excitatory postsynaptic potentials were recorded upon optical stimulation of the dentate gyrus. After recording, mice were perfused transcardially with PBS followed by 4% PFA. Brains were sectioned to check for the presence of retroviral-labeled adult-born neurons, and the sites of stimulation in dentate gyrus and recording in CA3 (Supplementary Fig. 3). Mice were excluded if the recording site was out of CA3. Slope of fEPSPs in each trace was measured and averaged every 2 minutes for analysis and plotting. For each animal, fEPSPs slope values in the last 15 minutes (45–60 min) were compared with baseline values (−20-0 min) by two-tailed independent t-test. Recording was considered a successful LTP if fEPSPs slope values in the last 15 minutes are siginificantly greater than baseline ($p<0.05$).

Fos immunohistochemistry and analysis

Neuronal activity during memory retrieval was analyzed by imaging immediate-early gene c-fos expression as previously discribed [24], and illustrated in Supplementary Fig. 9a. Briefly, ninety minutes following the completion of behavioral testing, mice were deeply anesthetized and perfused transcardially with PBS and then 4% paraformaldehyde (PFA). Brains were removed, fixed overnight in PFA and then transferred to 30% sucrose solution and stored at 4 °C. Brains were sectioned into 50 μm coronal sections covering the full anterior-posterior extent of the dentate gyrus. Immunohistochemistry was performed using primary antibodies to Fos (rabbit anti-Fos polyclonal antibody; 1:1,000, Calbiochem, Catalog# PC38), and Alexa-568 goat anti-rabbit (1:500, Molecular Probes, Catalog# A11011) as secondary antibodies. Sections were incubated in primary antibodies overnight, and then with secondary antibodies for 2 hours at room temperature, in the presence of 2% goat serum, 1% bovine serum albumin and 0.2% Triton X-100. Sections were mounted on slides with Permafluor anti-fade medium (Lipshaw Immunon). Images of the dentate gyrus were taken on an Olympus FLV1000 confocal microscope, and we quantified Fos+ and EGFP+/Arch + cells throughout the anterior-posterior extent of the granule cell layer. Number of Fos+ cells and EGFP+/Arch + cells quantify from two-dimensional images of the entire dentate gyrus, and the ratio of Fos+ in EGFP+/Arch+ cells was calculated for each animal.

Staining and reconstruction of biocytin-filled neurons

Brain sections with biocytin-filled neurons were fixed in 4% PFA overnight and stained using an alexa 647-conjugated streptavidin from Invitrogen. Images were acquired on an Olympus FLV1000 confocal system and biocytin-filled neurons were reconstructed afterwards using Olympus FluoView10 software.

Statistical analysis

Data were analyzed using ANOVAs followed by t-tests. Significance was considered when $p < 0.05$. ANOVAs and most t-tests are described in the figure captions. In the water maze, animals were considered to be searching selectively if percent search in NE was significantly greater than each of the other quadrants (i.e., NE>NW, NE>SE, NE>SW). If NE was not greater than all other quadrants the search was considered not selective. For all behavioral experiments, animals were randomly grouped and data analysis was blinded. Cell counting and c-fos analysis were blinded.

Supplementary Material

Refer to Web version on PubMed Central for supplementary material.

Acknowledgments

We thank Josef Bischofberger, Gary Matthews, Lorna Role and Hongjun Song for their critical comments, Qiaojie Xiong and Jason Tucciarone for technical support. We thank Fred Gage's laboratory for sharing their behavioral protocols. This work was supported by NIH (NS065915) and AHA (0930067N) grants to S.G. and Canadian Institutes of Health Research grants to P.W.F. (MOP86762) and S.A.J. (MOP74650).

References

1. Kempermann G, Gast D, Gage FH. Neuroplasticity in old age: sustained fivefold induction of hippocampal neurogenesis by long-term environmental enrichment. Ann Neurol. 2002; 52:135–143.10.1002/ana.10262 [PubMed: 12210782]
2. Ming GL, Song H. Adult neurogenesis in the mammalian brain: significant answers and significant questions. Neuron. 2011; 70:687–702. S0896-6273(11)00348-5 [pii]. 10.1016/j.neuron.2011.05.001 [PubMed: 21609825]
3. Cameron HA, McKay RD. Adult neurogenesis produces a large pool of new granule cells in the dentate gyrus. J Comp Neurol. 2001; 435:406–417. [PubMed: 11406822]
4. Kim WR, Christian K, Ming GL, Song H. Time-dependent involvement of adult-born dentate granule cells in behavior. Behav Brain Res. 2011 S0166-4328(11)00528-6 [pii]. 10.1016/j.bbr.2011.07.012
5. Aimone JB, Deng W, Gage FH. Resolving new memories: a critical look at the dentate gyrus, adult neurogenesis, and pattern separation. Neuron. 2011; 70:589–596. S0896-6273(11)00391-6 [pii]. 10.1016/j.neuron.2011.05.010 [PubMed: 21609818]
6. Sahay A, et al. Increasing adult hippocampal neurogenesis is sufficient to improve pattern separation. Nature. 2011; 472:466–470. nature09817 [pii]. 10.1038/nature09817 [PubMed: 21460835]
7. Arruda-Carvalho M, Sakaguchi M, Akers KG, Josselyn SA, Frankland PW. Posttraining ablation of adult-generated neurons degrades previously acquired memories. J Neurosci. 2011; 31:15113–15127.10.1523/JNEUROSCI.3432-11.2011 [PubMed: 22016545]
8. Drew MR, Denny CA, Hen R. Arrest of adult hippocampal neurogenesis in mice impairs single- but not multiple-trial contextual fear conditioning. Behav Neurosci. 2010; 124:446–454. 2010-16138-002 [pii]. 10.1037/a0020081 [PubMed: 20695644]
9. Snyder JS, Soumier A, Brewer M, Pickel J, Cameron HA. Adult hippocampal neurogenesis buffers stress responses and depressive behaviour. Nature. 2011; 476:458–461. nature10287 [pii]. 10.1038/nature10287 [PubMed: 21814201]
10. van Praag H, et al. Functional neurogenesis in the adult hippocampus. Nature. 2002; 415:1030–1034. 4151030a [pii]. 10.1038/4151030a [PubMed: 11875571]
11. Ge S, et al. GABA regulates synaptic integration of newly generated neurons in the adult brain. Nature. 2006; 439:589–593. nature04404 [pii]. 10.1038/nature04404 [PubMed: 16341203]
12. Esposito MS, et al. Neuronal differentiation in the adult hippocampus recapitulates embryonic development. J Neurosci. 2005; 25:10074–10086. 25/44/10074 [pii]. 10.1523/JNEUROSCI.3114-05.2005 [PubMed: 16267214]
13. Schmidt-Hieber C, Jonas P, Bischofberger J. Enhanced synaptic plasticity in newly generated granule cells of the adult hippocampus. Nature. 2004; 429:184–187. nature02553 [pii]. 10.1038/nature02553 [PubMed: 15107864]
14. Overstreet Wadiche L, Bromberg DA, Bensen AL, Westbrook GL. GABAergic signaling to newborn neurons in dentate gyrus. J Neurophysiol. 2005; 94:4528–4532. 00633.2005 [pii]. 10.1152/jn.00633.2005 [PubMed: 16033936]
15. Faulkner RL, et al. Development of hippocampal mossy fiber synaptic outputs by new neurons in the adult brain. Proc Natl Acad Sci U S A. 2008; 105:14157–14162. 0806658105 [pii]. 10.1073/pnas.0806658105 [PubMed: 18780780]
16. Toni N, et al. Neurons born in the adult dentate gyrus form functional synapses with target cells. Nat Neurosci. 2008; 11:901–907. nn.2156 [pii]. 10.1038/nn.2156 [PubMed: 18622400]
17. Zhao C, Teng EM, Summers RG Jr, Ming GL, Gage FH. Distinct morphological stages of dentate granule neuron maturation in the adult mouse hippocampus. J Neurosci. 2006; 26:3–11. 26/1/3 [pii]. 10.1523/JNEUROSCI.3648-05.2006 [PubMed: 16399667]
18. Hastings NB, Seth MI, Tanapat P, Rydel TA, Gould E. Granule neurons generated during development extend divergent axon collaterals to hippocampal area CA3. J Comp Neurol. 2002; 452:324–333.10.1002/cne.10386 [PubMed: 12355416]

19. Ge S, Yang CH, Hsu KS, Ming GL, Song H. A critical period for enhanced synaptic plasticity in newly generated neurons of the adult brain. Neuron. 2007; 54:559–566. S0896-6273(07)00334-0 [pii]. 10.1016/j.neuron.2007.05.002 [PubMed: 17521569]
20. Marin-Burgin A, Mongiat LA, Pardi MB, Schinder AF. Unique processing during a period of high excitation/inhibition balance in adult-born neurons. Science. 2012; 335:1238–1242.10.1126/science.1214956 [PubMed: 22282476]
21. Kee N, Teixeira CM, Wang AH, Frankland PW. Preferential incorporation of adult-generated granule cells into spatial memory networks in the dentate gyrus. Nat Neurosci. 2007; 10:355–362. nn1847 [pii]. 10.1038/nn1847 [PubMed: 17277773]
22. Tashiro A, Makino H, Gage FH. Experience-specific functional modification of the dentate gyrus through adult neurogenesis: a critical period during an immature stage. J Neurosci. 2007; 27:3252–3259. 27/12/3252 [pii]. 10.1523/JNEUROSCI.4941-06.2007 [PubMed: 17376985]
23. Nakashiba T, et al. Young dentate granule cells mediate pattern separation, whereas old granule cells facilitate pattern completion. Cell. 2012; 149:188–201.10.1016/j.cell.2012.01.046 [PubMed: 22365813]
24. Zhang F, et al. Multimodal fast optical interrogation of neural circuitry. Nature. 2007; 446:633–639. nature05744 [pii]. 10.1038/nature05744 [PubMed: 17410168]
25. Nagel G, et al. Channelrhodopsin-2, a directly light-gated cation-selective membrane channel. Proc Natl Acad Sci U S A. 2003; 100:13940–13945. 1936192100 [pii]. 10.1073/pnas.1936192100 [PubMed: 14615590]
26. Nicoll RA, Schmitz D. Synaptic plasticity at hippocampal mossy fibre synapses. Nat Rev Neurosci. 2005; 6:863–876. nrn1786 [pii]. 10.1038/nrn1786 [PubMed: 16261180]
27. Lin JY, Lin MZ, Steinbach P, Tsien RY. Characterization of engineered channelrhodopsin variants with improved properties and kinetics. Biophys J. 2009; 96:1803–1814. S0006-3495(09)00016-2 [pii]. 10.1016/j.bpj.2008.11.034 [PubMed: 19254539]
28. Gunaydin LA, et al. Ultrafast optogenetic control. Nat Neurosci. 2010; 13:387–392.10.1038/nn.2495 [PubMed: 20081849]
29. Alle H, Geiger JR. Combined analog and action potential coding in hippocampal mossy fibers. Science. 2006; 311:1290–1293. 311/5765/1290 [pii]. 10.1126/science.1119055 [PubMed: 16513983]
30. Yoshimura Y, et al. Involvement of T-type Ca2+ channels in the potentiation of synaptic and visual responses during the critical period in rat visual cortex. Eur J Neurosci. 2008; 28:730–743. EJN6384 [pii]. 10.1111/j.1460-9568.2008.06384.x [PubMed: 18657180]
31. Randall AD, Tsien RW. Contrasting biophysical and pharmacological properties of T-type and R-type calcium channels. Neuropharmacology. 1997; 36:879–893. S0028390897000865 [pii]. [PubMed: 9257934]
32. Snyder JS, Kee N, Wojtowicz JM. Effects of adult neurogenesis on synaptic plasticity in the rat dentate gyrus. J Neurophysiol. 2001; 85:2423–2431. [PubMed: 11387388]
33. Chow BY, et al. High-performance genetically targetable optical neural silencing by light-driven proton pumps. Nature. 2010; 463:98–102. nature08652 [pii]. 10.1038/nature08652 [PubMed: 20054397]
34. Morris RG, Garrud P, Rawlins JN, O'Keefe J. Place navigation impaired in rats with hippocampal lesions. Nature. 1982; 297:681–683. [PubMed: 7088155]
35. Kim JJ, Fanselow MS. Modality-specific retrograde amnesia of fear. Science. 1992; 256:675–677. [PubMed: 1585183]
36. Deng W, Aimone JB, Gage FH. New neurons and new memories: how does adult hippocampal neurogenesis affect learning and memory? Nat Rev Neurosci. 2010; 11:339–350. nrn2822 [pii]. 10.1038/nrn2822 [PubMed: 20354534]
37. Bezprozvanny I, Tsien RW. Voltage-dependent blockade of diverse types of voltage-gated Ca2+ channels expressed in Xenopus oocytes by the Ca2+ channel antagonist mibefradil (Ro 40-5967). Mol Pharmacol. 1995; 48:540–549. [PubMed: 7565636]
38. Bergquist F, Nissbrandt H. Influence of R-type (Cav2.3) and t-type (Cav3.1-3.3) antagonists on nigral somatodendritic dopamine release measured by microdialysis. Neuroscience. 2003; 120:757–764. S0306452203003853 [pii]. [PubMed: 12895515]

39. Kerr AM, Jonas P. The two sides of hippocampal mossy fiber plasticity. Neuron. 2008; 57:5–7. S0896-6273(07)01025-2 [pii]. 10.1016/j.neuron.2007.12.015 [PubMed: 18184559]

40. Ge S, Sailor KA, Ming GL, Song H. Synaptic integration and plasticity of new neurons in the adult hippocampus. J Physiol. 2008; 586:3759–3765.10.1113/jphysiol.2008.155655 [PubMed: 18499723]

41. Sahay A, Wilson DA, Hen R. Pattern separation: a common function for new neurons in hippocampus and olfactory bulb. Neuron. 2011; 70:582–588. S0896-6273(11)00393-X [pii]. 10.1016/j.neuron.2011.05.012 [PubMed: 21609817]

42. Teixeira CM, Pomedli SR, Maei HR, Kee N, Frankland PW. Involvement of the anterior cingulate cortex in the expression of remote spatial memory. J Neurosci. 2006; 26:7555–7564. 26/29/7555 [pii]. 10.1523/JNEUROSCI.1068-06.2006 [PubMed: 16855083]

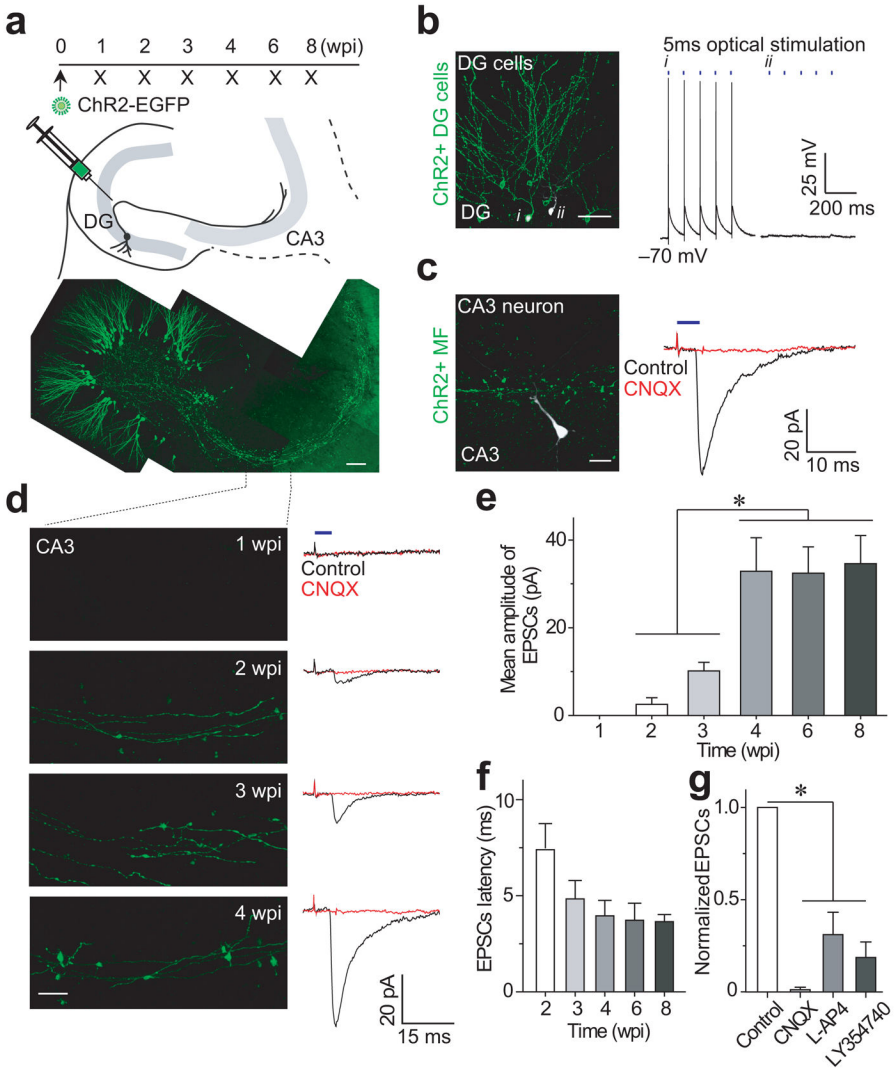

Figure 1. Adult-born neurons form functional synapses on CA3 pyramidal neurons

(a) Upper: Experimental timeline. Lower: Image showing adult-born DGCs (4 wpi) and their axons (EGFP$^+$). Scale bar: 50 μm. **(b)** Light pulses (473 nm, 5 ms) elicit action potentials in ChR2-EGFP-infected, but not neighboring (EGFP) DGCs. Left: Image showing recorded DGCs filled with biocytin (white) in an acute brain slice (4 wpi). *i*, a ChR2-EGFP$^+$ newborn neuron (green and white); *ii*, a non-infected neighbor (white). Scale bar: 50 μm. Right: Light induced action potentials in EGFP$^+$ (*i*) but not in EGFP$^-$(*ii*) DGC. **(c)** Optically-evoked EPSCs from adult-born DGCs. Left: Image showing ChR2-EGFP$^+$ axonal terminals (green) of adult-born DGCs (4 wpi) and a recorded CA3 pyramidal neuron (white). Scale bar: 25μm. Right: a sample optically-evoked EPSCs recorded from this cell, subsequently blocked by 50 μM CNQX. **(d)** Axon integration (left, EGFP) and formation of functional synapses on CA3 neurons (right) at 1, 2, 3 and 4 wpi. Scale bar: 10 μm. **(e)** Amplitude of EPSCs at 1, 2, 3, 4, 6 and 8 wpi ($p<0.05$; n=5–15 cells, two-tailed unpaired t-test). **(f)** Latency of EPSCs at 2, 3, 4, 6 and 8 wpi. **(g)** Shown is a summary of EPSCs which were inhibited by 50μM L-AP4 (t=5.465, p=0.012; n=5 cells, two-tailed paired t-test) or

1μM LY354740 (t=3.891, p=0.027; n=6 cells, two-tailed paired t-test), and blocked by 50μM CNQX (t=5.835, p=0.007; n=15 cells, two-tailed paired t-test). All values represent mean±SEM (*, $p<0.05$).

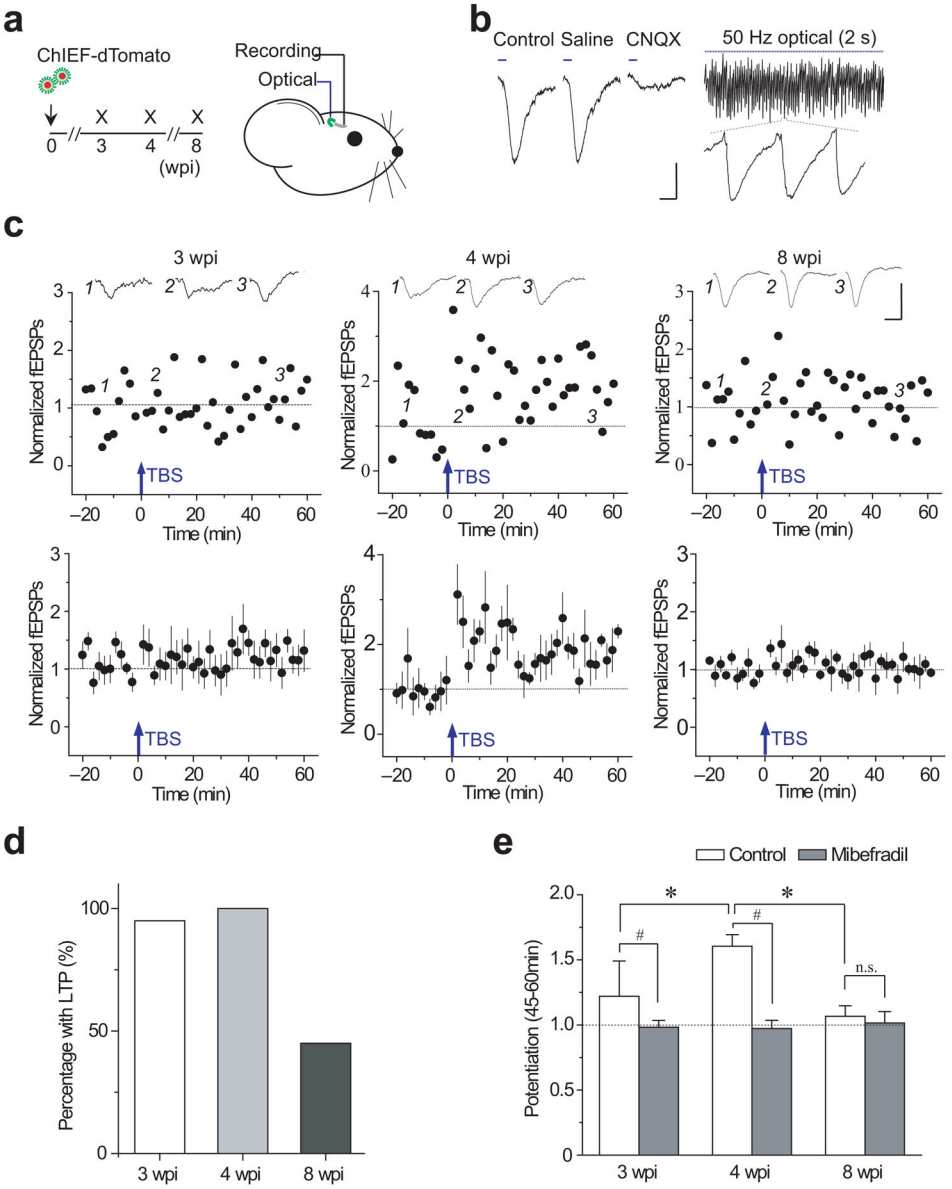

Figure 2. Adult-born neurons at 4 weeks of age show enhanced plasticity at output synapses

(a) Experimental timeline. **(b)** Optically stimulating adult-born neurons produces fEPSPs in the CA3 area. Left, fEPSPs blocked by infusion of 50μM CNQX (but not saline). Right, optical stimulation (50 Hz pulses of 5 ms) reliably induced fEPSPs. Scale bars: 5 ms and 0.1 mV. **(c)** Theta-burst optical stimulation of adult-born neurons produces LTP at CA3 synapses in an age-dependent manner. Top row, examples of fEPSPs LTP from a single animal at 3, 4 or 8 wpi. Insets: Averaged traces of fEPSPs from 5 consecutive recordings before (*1*), immediately following (*2*), and after (*3*) LTP induction using TBS (blue arrow, Supplementary Fig. 2). Shown at the bottom is a summary of LTP from groups of animals, respectively. **(d)** Percentage of mice (3, 4 and 8 wpi) exhibiting reliable LTP. **(e)** Summary of the mean potentiation of fEPSPs amplitude 45–60 min following TBS from mice under control condition (3, 4 and 8 wpi with 6, 8 and 8 animals, respectively; t-test between

groups: 3 vs. 4 wpi t=3.386, p=0.007; 8 vs. 4 wpi, t=4.483, p=0.002) or after application of mibefradil (25mg/kg, i.p.) (t-test between control and mibefradil conditions: 3 wpi, t=3.823, p=0.007, n=4; 4 wpi, t=5.656, p<0.001, n=5; 8 wpi, t=0.954, p=0.41, n=4). In each group, all animals tested with stable baseline were included. All values represent mean±SEM (both * and # mean p<0.05; n.s., p>0.05; n is the number of animals; two-tailed unpaired t-test).

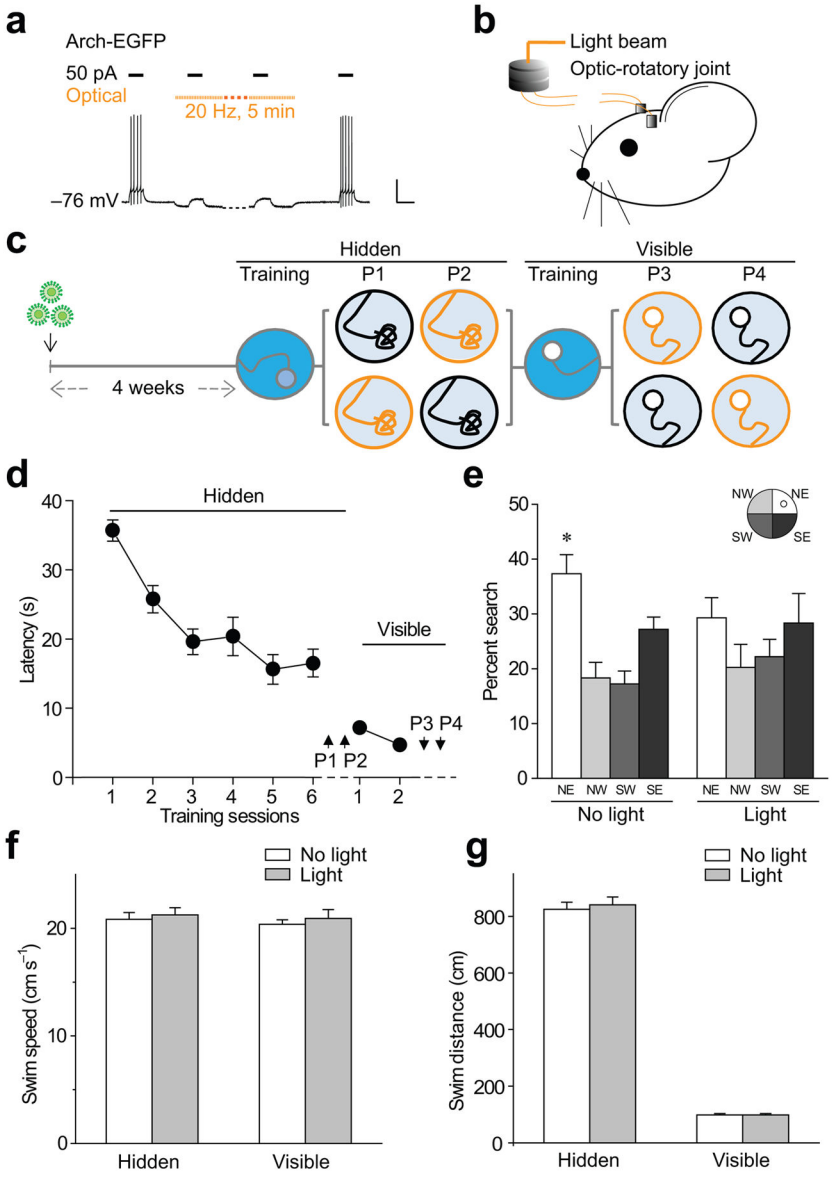

Figure 3. Reversibly silencing 4 week-old adult-born neurons impairs hippocampal memory retrieval

(a) Optical stimulation (589 nm) silences Arch-EGFP expressing adult-born neurons. Scale bars: 100 ms and 30 mV. **(b)** Schematic drawing showing a mouse with implanted optrodes connected to an orange light source via optic fibers and an optic rotatory joint. **(c)** Time-line of watermaze experiment. **(d)** Animals were trained with no light. Shown is the training curve of latency to find the platform. **(e)** Optically inactivating a cohort of 4 week-old adult-born neurons impaired hippocampal memory retrieval. During the probe, mice in the “no light” condition spent significantly more time searching in the target quadrant (NE) compared to the other quadrants: (One-way repeated measures ANOVA $F_{3,39}$=7.139, p<0.001; NE>NW, SW, SE by paired t-test planned comparison, n=14), showing robust spatial memory. In contrast, mice in the “light” condition (inactivation) didn’t spend significantly more time in NE compared to other quadrants ($F_{3,39}$=0.9655, p=0.4187; p>0.05

NE vs. NW, SW, SE; n=14), showing a disruption of spatial memory ($NE_{no\ light}$>NE_{light} t=2.153, p=0.0253 by planned comparison). **(f)** Optical inactivation did not alter swim speed in hidden probe tests (P1 and P2, t=1.046, p=0.3145; n=14) and visible probe tests (P3 and P4, t=0.6464, p=0.2646; n=14). **(g)** Optical inactivation did not alter swim distance in hidden probe tests (P1 and P2, t=1.008, p=0.1660; n=14) and visible probe tests (P3 and P4, t=0.0173, p=0.09867; n=14). All values represent mean±SEM (*: p<0.05; one-way ANOVA or two-tailed t-test).

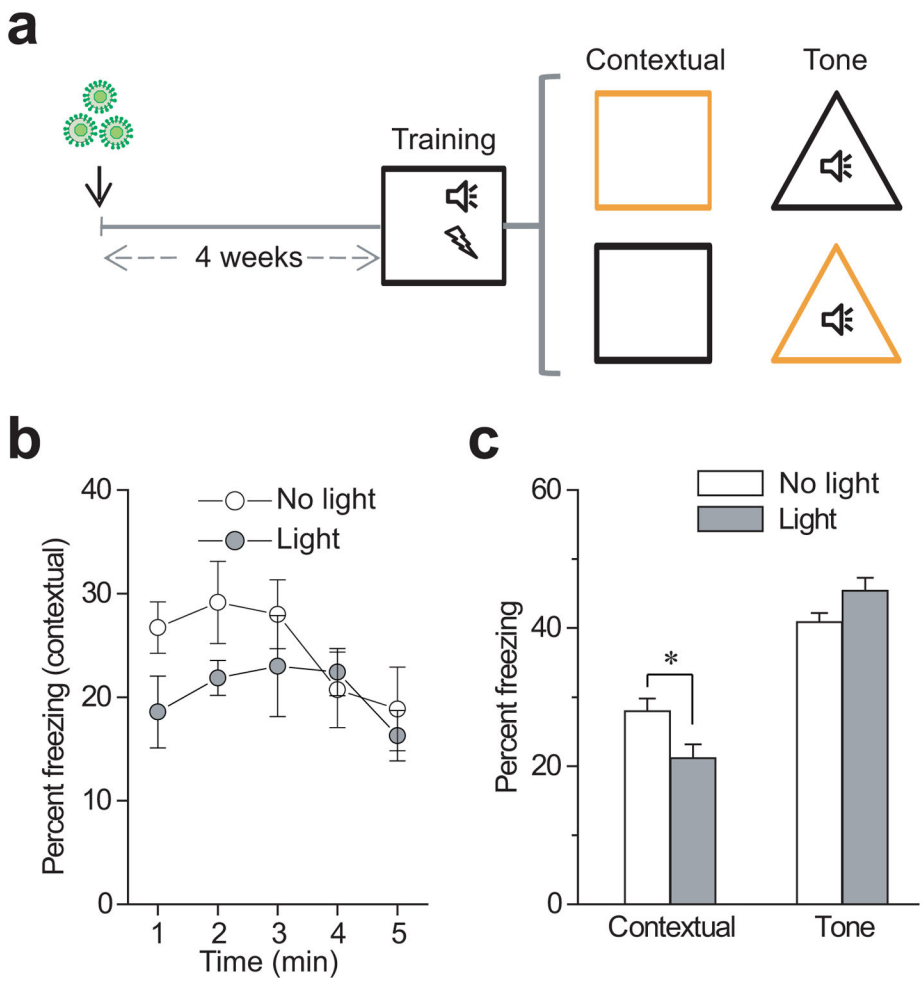

Figure 4. Temporary silencing of 4 week-old newborn neurons impairs expression of a fear conditioning memory

(a) Time-line of fear conditioning test. Adult mice were infused with a retroviral vector (Arch-EGFP), implanted with optrodes and trained in fear conditioning (single tone-shock pairing). Twenty-four hours after training, contextual fear memory was assessed. An additional tone test was performed in which mice were placed in a novel context and the tone replayed. Animals were divided into two groups and optical silencing was counterbalanced in contextual and tone freezing tests. **(b)** Silencing of adult-born DGCs at 4 wpi reduced freezing to the context compared to control (n=7, 7). **(c)** Optically inactivating adult-born DGCs at 4wpi reduced freezing to the context (first 2 minutes of the context test, t=2.239, p=0.0224; n=7, 7), but had no effect on tone fear memory (t=1.675, p=0.0599; n=7, 7). To avoid potential interference from with-in session extinction, we measured freezing time in the first 2 minutes. All values represent mean±SEM (*: $p<0.05$, two-tailed t-test).

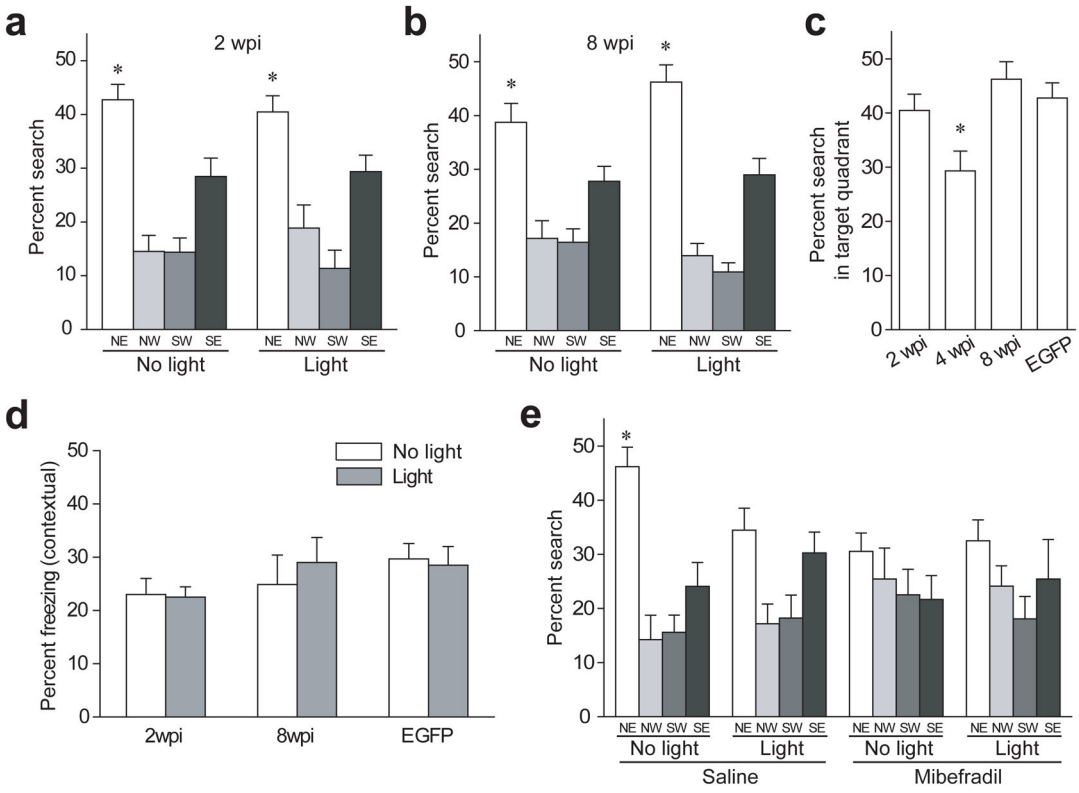

Figure 5. Behavioral roles of adult-born DGCs is sensitive to their age

(a–b) Silencing adult-born DGCs at 2 or 8 wpi showed no significant effect on memory retrieval. Mice at 2 (**a**) or 8 (**b**) wpi spent more time searching in the target quadrant (NE) compared to the other quadrants in both "no light" (One-way repeated measures ANOVA 2 wpi: $F_{3,15}$=15.25, p<0.0001; 8 wpi: $F_{3,15}$=8.081, p=0.0019; NE>NW, SW, SE by paired t-test planned comparison in both; n=6,6) and "light" conditions (2 wpi: $F_{3,15}$=9.125, p=0.0011; 8 wpi: $F_{3,15}$=14.20, p=0.0001; NE>NW, SW, SE in both; n=6, 6). **(c)** Silencing adult-born DGCs impacted memory retrieval age-dependently. 4 wpi group showed significant less time searching in target quadrant in "light" condition (n=14) comparing to 2 (n=6, t=2.360, p=0.030), 8 wpi (n=6, t =2.922, p=0.0135), and EGFP 4 wpi (n=8, t=2.392, p=0.0286) by two-tailed unpaired t-test. **(d)** Silencing of adult-born DGCs at 2 or 8 wpi failed to affect fear memory retrieval. Percent freezing of Arch animals at 2 (t=0.2029, p=0.4246; n=5), 8 wpi (t=0.3824, p=0.3568; n=8) or EGFP at 4 wpi (t=0.4593, p=0.3326; n=6). Two-tailed paired t-test comparison was made between "no light" and "light" conditions. **(e)** Mibefradil prevented hippocampal memory retrieval of the animals at 4 wpi. Shown is a summary similar to those in (a) ($Saline_{No\ light}$: $F_{3,9}$=10.43, p=0.0027; NE>NW, SW, SE; $Saline_{Light}$: $F_{3,9}$=2.849, p=0.0975; $Mibefradil_{No\ light}$: $F_{3,9}$=1.173, p=0.3730; $Mibefradil_{Light}$: $F_{3,9}$=1.061, p=0.4128; n=4,4 for all). All values represent mean±SEM (*: p<0.05; n is the animal number, one-way ANOVA or two-tailed t-test).

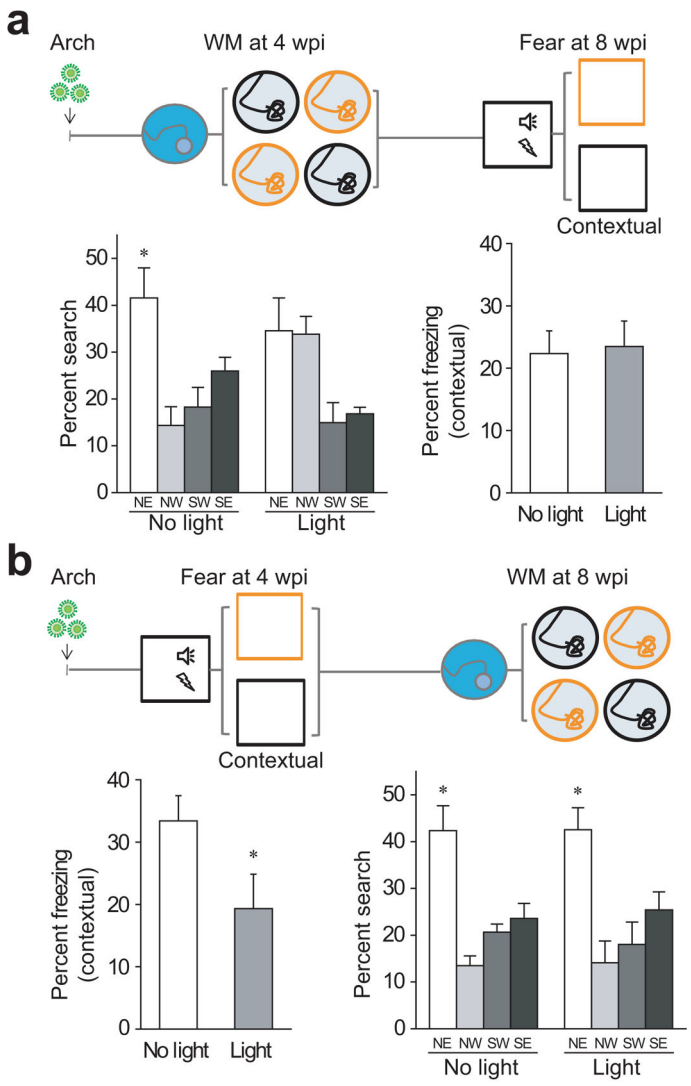

Figure 6. Task-switching experiments showing that adult-born DGCs at 4 wpi are important for memory retrieval

(a) Upper: Timeline of watermaze and fear conditioning tests. Lower panel: At 4 wpi, watermaze trained animals under the "no light" condition searched selectively (ANOVA $F_{3,12}$=9.487, p=0.0017; NE>NW, SW, SE; n=5, 5; Refers the analysis to Figs. 3–5), whereas in the "light" condition they failed to search selectively ($F_{3,12}$=4.004, p=0.0345; NE vs. NW t=0.0702, p=0.43; NE vs. SW t=1.792, p=0.077). When trained in the contextual fear conditioning at 8 wpi, animals displayed a similar percent freezing (t=0.3600, p=0.3685). **(b)** Upper: Time-line of fear conditioning and watermaze tests. Similar experiments have been performed to those in (a), but the order of behavioral tests has been switched: first fear condition and second watermaze. Lower panel: animals showed a significant decrease in percent freezing (t=3.046, p=0.0191) when trained at 4 wpi. However, at 8wpi, both No light and Light groups showed intact watermaze memory (No light: $F_{3,12}$=14.48, p=0.0003; Light: $F_{3,12}$=9.644, p=0.0016; NE>NW, SW, SE; n=5, 5). All values represent mean±SEM (*: p<0.05; n is the number of animals, one-way ANOVA or two-tailed paired t-test).